Physica A 414 (2014) 340–351

Contents lists available at ScienceDirect

Physica A

journal homepage: www.elsevier.com/locate/physa

Using the informational Fisher–Shannon method to investigate the influence of long-term deformation processes on geoelectrical signals: An example from the Taiwan orogeny

Luciano Telesca [a,*], Michele Lovallo [b], Gerardo Romano [a], Konstantinos I. Konstantinou [c], Han-Lun Hsu [c], Chien-chih Chen [c]

[a] Consiglio Nazionale delle Ricerche, Istituto di Metodologie per l'Analisi Ambientale, C.da S.Loja, 85050 Tito (PZ), Italy

[b] ARPAB, 85100 Potenza, Italy

[c] Institute of Geophysics, National Central University, Jhongli, Taoyuan, Taiwan

HIGHLIGHTS

- Time dynamics of geoelectrical signals could be linked with deformation processes.
- Three sites in Taiwan with different amounts of crustal deformation are investigated.
- The three sites are discriminated by using the Fisher–Shannon method.
- The differential strain intensity is correlated with the Fisher–Shannon quantities.

ARTICLE INFO

Article history:
Received 1 May 2014
Received in revised form 15 July 2014
Available online 24 July 2014

Keywords:
Geoelectrical signals
Taiwan
Deformation
Fisher information measure
Shannon entropy

ABSTRACT

The time dynamics of geoelectrical signals measured at three sites in Taiwan were investigated by using the Fisher–Shannon method in order to investigate the possible correlation between their properties with deformation processes. The three sites are located along an almost perpendicular direction to the orogenic collision zone where each site experiences different amounts of crustal deformation. Our findings point out to a clear discrimination of the three sites on the basis of the informational properties of the recorded geoelectrical signals. In particular a relationship is found between the differential strain intensity of the sites where the geoelectrical stations are located and the Fisher–Shannon quantities.

1. Introduction

The plate configuration near Taiwan is characterized by the oblique convergence of two plates, namely the Philippines Sea Plate (PSP) and the Eurasian Plate (EUP) at a rate of 8 cm/year in a direction of N310E [1] (Fig. 1). The Taiwan orogeny is the direct consequence of this convergence expressed by the collision of the Luzon volcanic arc in the PSP and the Chinese continental margin in the EUP which began 3–6 Ma [2–4]. This collision results in high crustal deformation and seismicity rates which are most intense along the eastern part of the island and progressively dissipate once one moves towards the

* Corresponding author. Tel.: +39 0971427277.
E-mail address: luciano.telesca@imaa.cnr.it (L. Telesca).

http://dx.doi.org/10.1016/j.physa.2014.07.060
0378-4371/

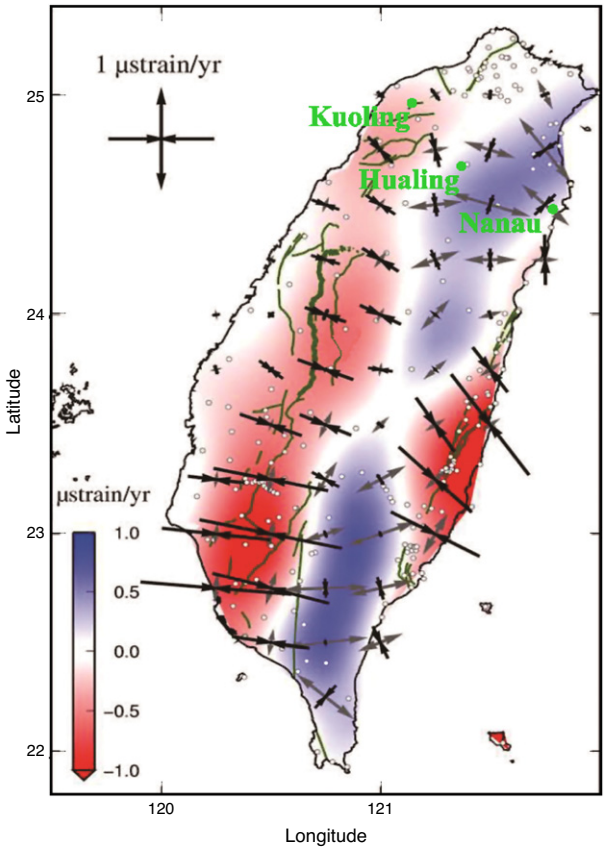

Fig. 1. Map of geoelectrical stations with strain rate field of Taiwan from GPS data between 1993 and 1999 (after Hsu 2009).

west. Present day deformation in Taiwan has been studied using both campaign and continuous GPS data augmented by geological observations [1,5–7] leading to a relatively detailed mapping of the stress/strain field.

Geoelectrical prospecting has long been used in geophysics for tectonic (e.g., faults) and environmental (e.g., in mapping waste disposal areas) applications by means of locating structures that exhibit anomalous electrical conductivities [8–10]. A more controversial application is the identification of anomalous patterns in geoelectrical signals prior to the occurrence of large earthquakes [48,11–19]. These patterns are thought to result from the deformation of the rock during the nucleation stage of the earthquake [45,20,21], thus it has been argued that they could be used as a short-term precursor [22–28]. If these short-term deformation variations are indeed reflected in the properties of geoelectrical signals, then this poses the question of whether longer term deformation variations have any influence on their properties as well.

Vallianatos and Tzanis [48] already investigated the proportionality between the electric field and the deformation rate. Our study extends such idea by elucidating the informational properties of geoelectrical signals recorded for a period of six months at three sites that span the deformation front of the Taiwan orogeny (Fig. 1). First, we give an overview of the data recording and their spectral characteristics. Then we proceed with the application of two methodologies, namely the Fisher Information Measure (FIM) and the Shannon Entropy that can provide information about the degree of order in observational data. Finally, the results along with the discussion follow.

2. Data

We measured the continuous self-potential (SP) data with 15 Hz sampling rate and GPS time correction at three sites across northern Taiwan from May to November 2012 (Fig. 1). These sites form a profile along a NW–SE direction where the crustal deformation varies in intensity and gradually switches from extensional in the area of the Ilan plain to compressional along the NW coastal plain of Taiwan [7]. The SP measurements at each site were the potential difference of two dipoles in North–South and East–West directions with length 1.89 and 3.57 km in Kuoling (Coastal Plain), 4.29 and 1.83 km in Hualing (Central Range), and 0.99 and 1.93 km in Nanau (south of Ilan plain). The daily fluctuations of NS and WE direction at Kuoling were 11.4 and 20.7, at Hualing were 147.3, 121.5 and Nanau were 30.5 and 43.1 mV/km. Those non-polarized electrodes ($Pb/PbCl_2$) were buried at 1 m depth and connected with the local telephone cable to each recording office. Then, the SP signals were converted to electric field and the minute averages were calculated (Fig. 2). In order to study the frequency

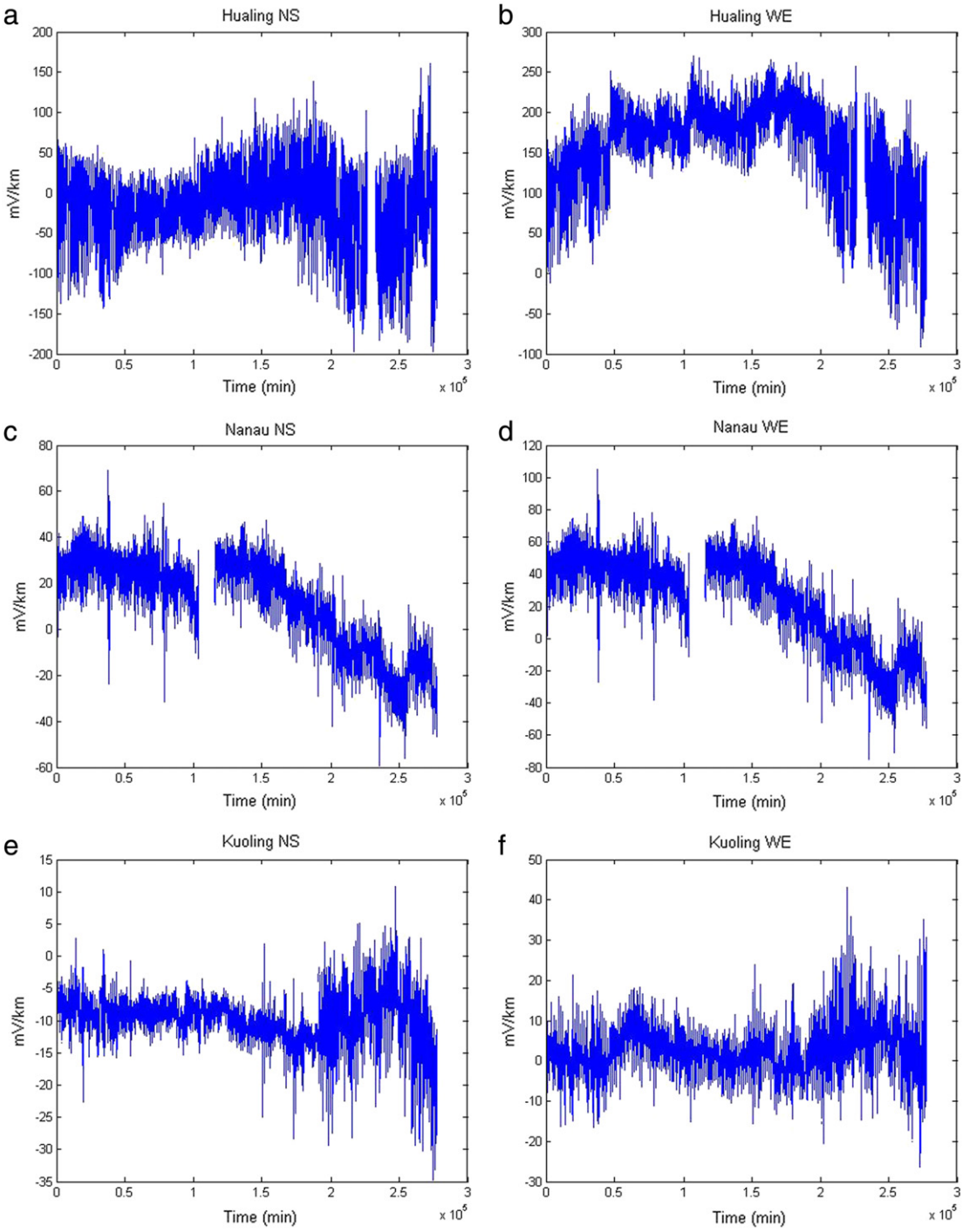

Fig. 2. Original data measured at Hualing (a, b), Nanau (c, d) and Kuoling (e, f) stations. The data are electric field measured in north–south (NS) and east–west (EW) directions.

content of the recorded signals, because of the presence of missing data in the series we employed the Lomb method to estimate the power spectral density [29]. Fig. 3 shows the Lomb spectra of the six signals: especially Hualing and Nanau are characterized by the presence of an intense daily cycle; also higher harmonics are visible, but less intense than the daily periodicity. Considering the high anthropization level of the monitored areas, the most reasonable source of the observed daily cyclicity has to be searched in the strong presence of cultural EM noise.

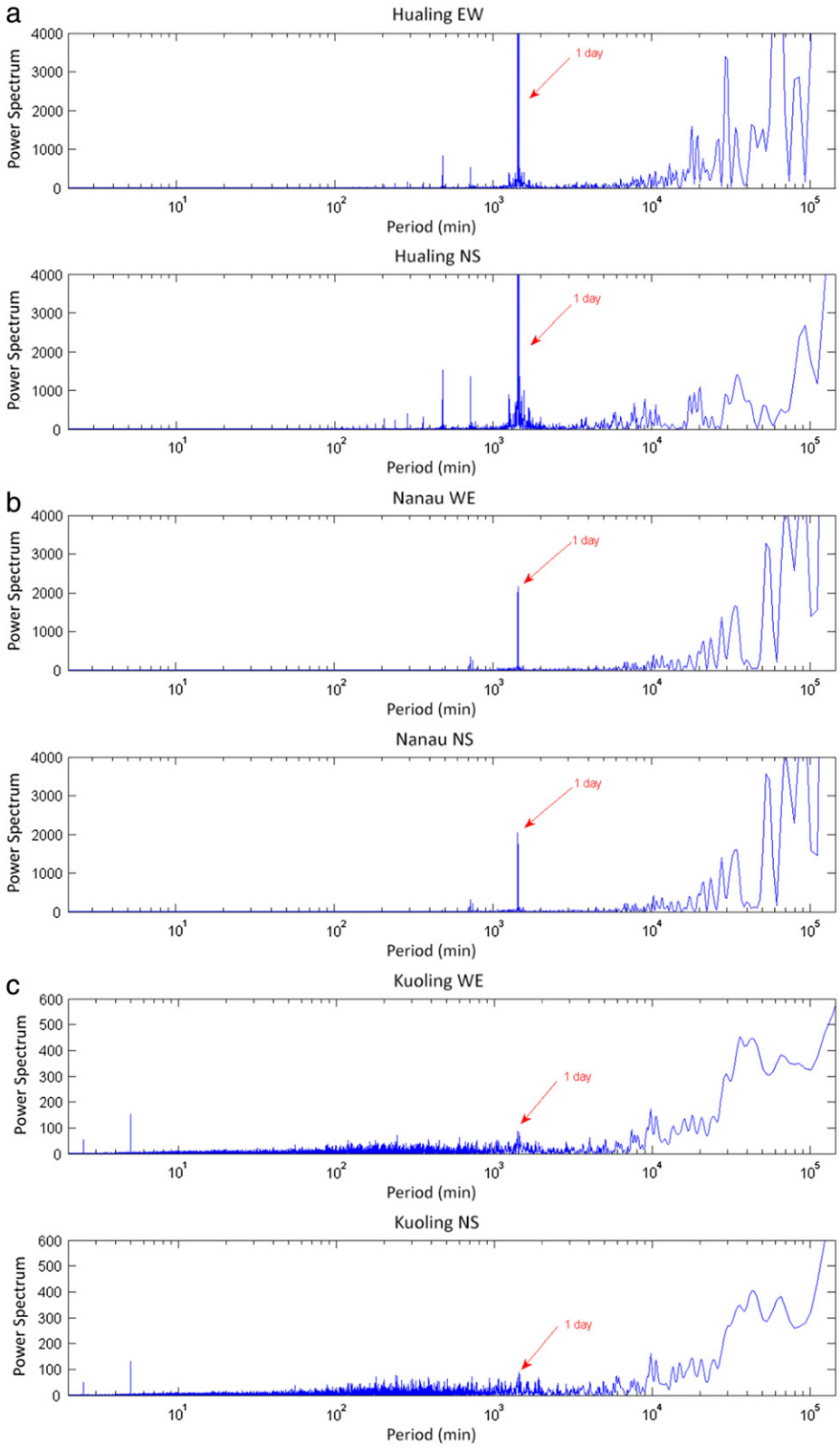

Fig. 3. Lomb spectra of the recorded signals shown in Fig. 2.

3. Method

The Fisher Information Measure (FIM) and the Shannon entropy are considered efficient methods for the investigation of the complex time dynamics in nonstationary time series. The FIM quantifies the degree of organization or order of a time series, while the Shannon entropy that of uncertainty or disorder [30]. The FIM was firstly proposed by Fisher [31] in the framework of the theory of statistical estimation. But, afterward, it was used in many scientific fields and with different aims, like the description of the evolution laws of physical systems [32], the characterization of the temporal fluctuations in electroencephalographic signals and detection of significant dynamical changes [33]. Several complex geophysical and environmental phenomena were studied using the FIM and the Shannon entropy to get information about the mechanisms governing their time dynamics and detect precursory features of critical phenomena [34–37]. Recently Telesca et al. [38,39] have employed the FIM to discriminate between tsunamigenic and non-tsunamigenic earthquake seismograms.

Let $f(x)$ be the probability density of a signal x, then its FIM I is given by

$$I = \int_{-\infty}^{+\infty} \left(\frac{\partial}{\partial x} f(x) \right)^2 \frac{\mathrm{d}x}{f(x)}, \tag{1}$$

and its Shannon entropy is defined as [30]:

$$H_X = -\int_{-\infty}^{+\infty} f(x)\ \log f\ (x)\ \mathrm{d}x. \tag{2}$$

For continuous distributions the Shannon entropy can take any real positive and negative value. In order to avoid the difficulty arising with negative information measures, the so-called Shannon power entropy N_X can be used instead of the Shannon entropy:

$$N_X = \frac{1}{2\pi e} \mathrm{e}^{2H_X}. \tag{3}$$

The calculation of the FIM and the Shannon entropy depends on the calculation of the probability density function $f(x)$ (pdf). The pdf can be estimated by means of the kernel density estimator technique [40,41] that approximates the density function as

$$\hat{f}_M(x) = \frac{1}{Mb} \sum_{i=1}^{M} K\left(\frac{x - x_i}{b} \right), \tag{4}$$

with b the bandwidth, M the number of data and $K(u)$ the kernel function, a continuous non-negative and symmetric function satisfying the two following conditions

$$K(u) \geq 0 \quad \text{and} \quad \int_{-\infty}^{+\infty} K(u)\mathrm{d}u = 1. \tag{5}$$

In our study, we estimated the pdf $f(x)$ by means of the algorithm developed in Ref. [42] combined with that developed in [43], that uses a Gaussian kernel with zero mean and unit variance:

$$\hat{f}_M(x) = \frac{1}{M\sqrt{2\pi b^2}} \sum_{i=1}^{M} \mathrm{e}^{-\frac{(x-x_i)^2}{2b^2}}. \tag{6}$$

4. Results and discussion

We calculated the FIM and the Shannon entropy power for the geoelectrical signals measured at the three stations of Kuoling, Hualing and Nanau. The results show that Nanau data are characterized by higher FIM and lower Shannon entropy power, while Kuoling data by higher Shannon entropy power and lower FIM (Figs. 4 and 5). This indicates that the structure of the time variation of Nanau data is more organized and ordered than that of Kuoling data. Hualing data are characterized by organization and order degree intermediate between those of the other two geoelectrical series. The Fisher–Shannon information plane, shown in Fig. 6, makes more evident the pattern given by the six datasets (three in NS and three in EW directions): a striking decreasing trend is visible between FIM and N_X among the three stations, where Nanau occupies the top left part of the plane and Kuoling the right bottom part.

A comparison with the data of differential strain intensity (DSI) [5] suggests a rather good correlation with the Fisher–Shannon results (Figs. 7 and 8): Kuoling station is located in a site with DSI $= 1.309 \cdot 10^{-7}$/year, Hualing station in a site with DSI $= 2.610 \cdot 10^{-7}$/year and Nanau with DSI $= 4.646 \cdot 10^{-7}$/year. Merging the FS results with the DSI data, it is observed that the Shannon entropy power decreases with the increase of DSI, while the FIM increases.

In order to check if the obtained results could depend on the presence of the daily cycle, we filtered the data with a low-pass filter with frequency cutoff at 1/(2 days), thus retaining only the low frequency part of the data and filtering out the daily

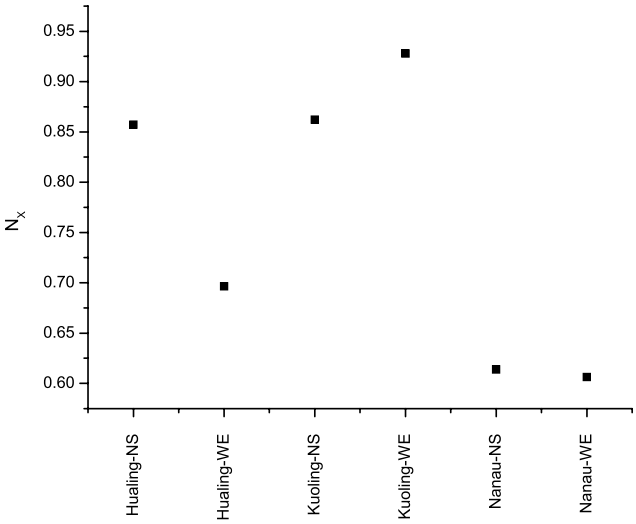

Fig. 4. Shannon entropy power of the six signals shown in Fig. 2.

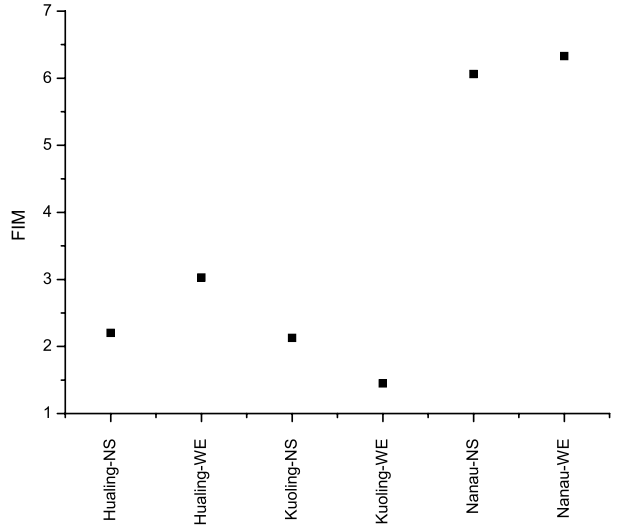

Fig. 5. FIM of the six signals shown in Fig. 2.

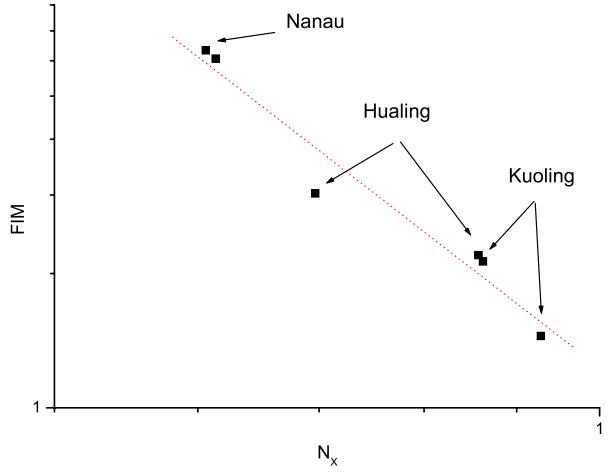

Fig. 6. Fisher–Shannon information plane of the six signals shown in Fig. 2.

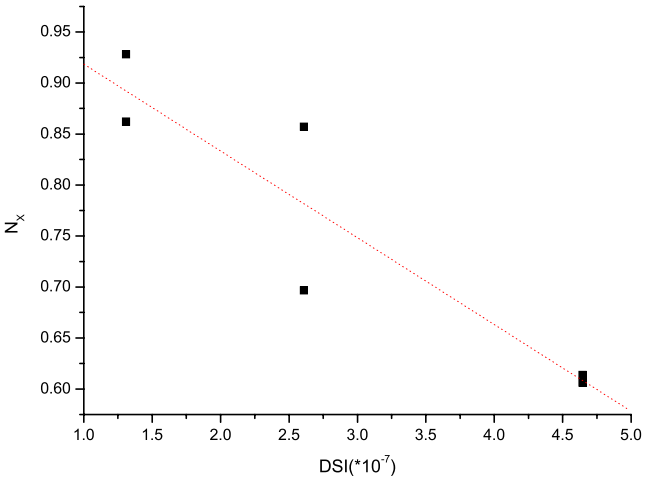

Fig. 7. Relationship between the Shannon entropy power for the signals shown in Fig. 2 and the DSI.

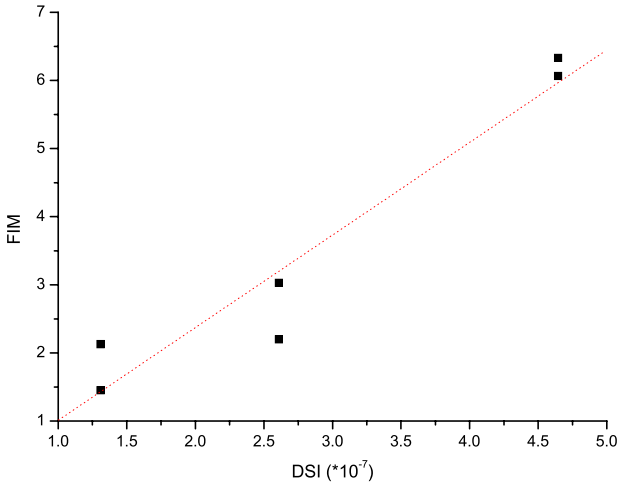

Fig. 8. Relationship between the FIM of the signals shown in Fig. 2 and the DSI.

cycle and its higher harmonics. The normalized (after subtracting the mean and dividing for the standard deviation) residual signals are shown in Fig. 9. We applied the FS method to such residual signals and the results are shown in Figs. 10–14. It can be observed that the Shannon entropy power (Fig. 10) and FIM (Fig. 11) are still the lowest and the highest, respectively, for Nanau, which occupies the left upper part of the FS plane (Fig. 12), similarly to the original not filtered data. Therefore, the FS pattern evidences a decreasing trend similarly to that shown by the original data. Even the relationship between the N_X (FIM) and the DSI preserves the same behavior as obtained for the original data (Figs. 13 and 14). All these features indicate that the FS results depend mainly on the low-frequency content of the signals and are robust against the presence of daily periodicities, even very intense.

We see that there is a significant difference in the FIM and N_X values between the NS and WE components at Hualing station; this difference could be due to the different nature of the data recorded along the NS and WE directions. As we can see in Fig. 3, the Lomb spectrum of the WE component in Hualing, particularly for the periods longer than 2 days, is largely different from that one of the NS component while the spectra along two directions show much more similarity in both Nanau and Kuoling stations. This is also evident that we have larger deviation in the N_X values of the NS and WE components to the low-passed data as shown in Fig. 12. Therefore, it is not surprising that the FIM and N_X values for EW and NS are close to Nanau and Kuoling stations.

It is striking the nice relationship between the informational quantities calculated for the signals and the differential strain intensity (DSI). The DSI is defined as the absolute difference between the two eigenvalues of the horizontal strain tensor [5], and is calculated from the GPS data; thus, in a certain sense, it represents a quantitative measure of "deformation intensity". Mechanically speaking, a higher DSI indicates a stronger tendency that crustal deformation occurs mainly along some preferred direction, thus very likely builds up some kind of orientation-preferred structures in the crust. Rocks subject to high differential stress are usually deformed and a mineral-preferred orientation could then develop by one of the

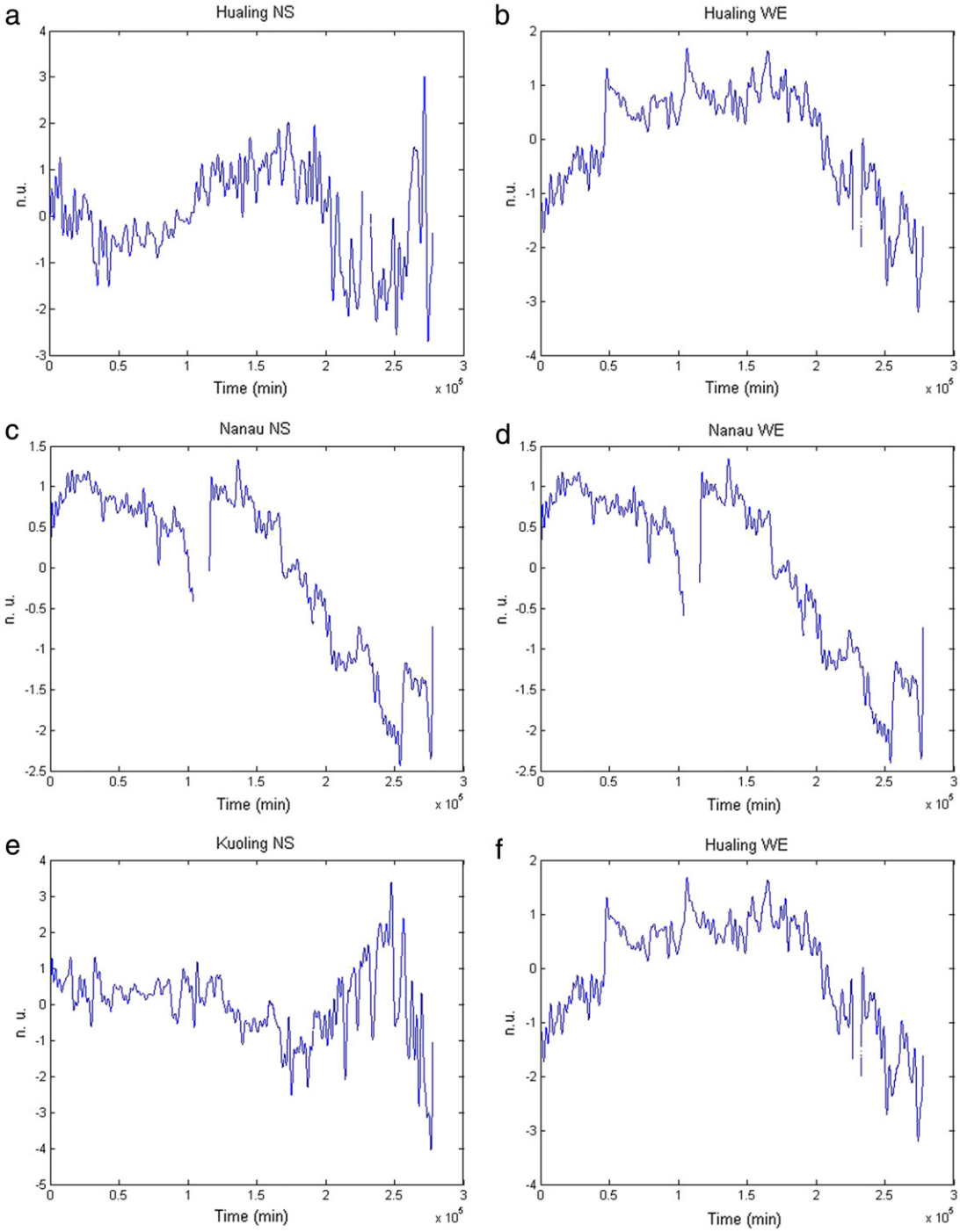

Fig. 9. Normalized residuals after filtering the data with a low-pass filter with frequency cutoff at 1/(2days).

processes like recrystallization, solution transfer, mechanical rotation and so on. On the other side, it could be argued that a lower DSI indicates that the crustal deformation occurs in both directions with rather similar intensity, and one direction is not "dominant" on the other. Note that the dynamics of the time variation in the geoelectrical data at the Nanau station, with a relatively higher DSI, is more organized and ordered (higher FIM and lower N_X) than that of data measures at Kuoling site that is characterized by a relatively lower DSI. Therefore, possibly, such kind of orientation-preferred structures in a systematic way organize and order the geoelectrical data, as indicated by the higher FIM and lower Shannon entropy power at the Nanau station.

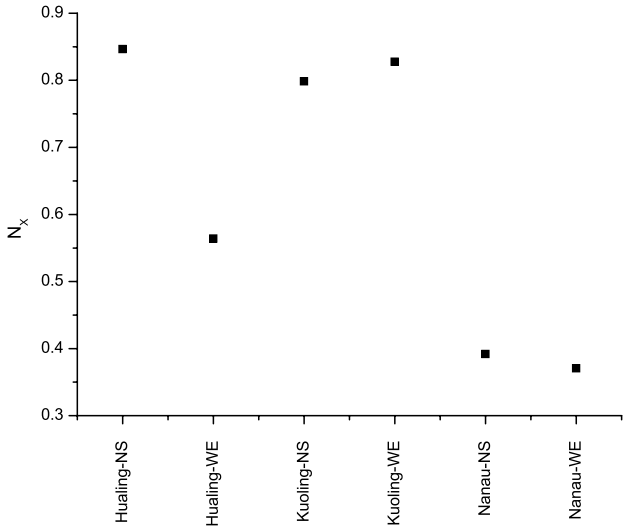

Fig. 10. Shannon entropy power of the six residual signals shown in Fig. 9.

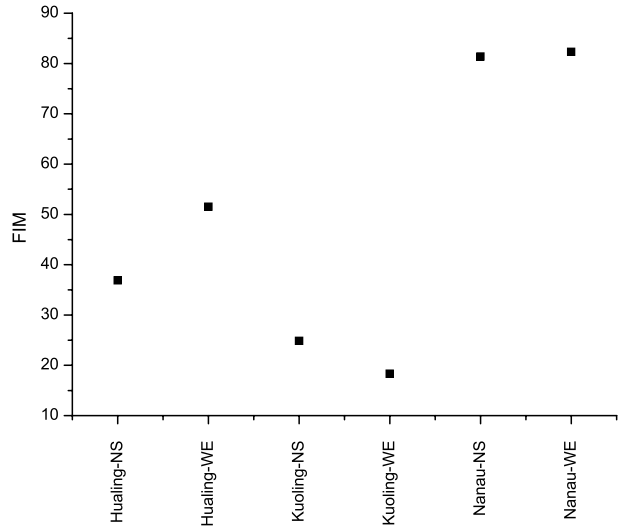

Fig. 11. FIM of the six signals shown in Fig. 9.

5. Conclusions

Our investigation of the influence of long-term deformation processes on geoelectrical signals shows a clear correlation between their information properties and the differential deformation intensity along the Taiwan orogeny. Previously, piezoelectric and electrokinetic phenomena have been invoked for the purpose of explaining the generation of precursory and co-seismic geoelectrical signals (e.g. Ref. [44]). Also piezoelectric models combined with the dislocation theory of a fault model [47], and electrokinetic models taking into account finite fault planar models [46] were considered.

The signals generated by such processes however, correspond to much shorter time scales than the time scale represented by the low frequency content of the signals we have studied. In this sense our results cannot be explained by a simple piezoelectric effect prior to rock failure, but rather imply that another physical process may connect the buildup of differential strain with geoelectrical signal generation in areas of intense deformation like Taiwan. This suggestion is also supported by laboratory experiments involving the progressive deformation of quartz-free rocks that revealed the generation of Pressure Stimulated Currents (PSC) [27]. A larger amplitude of PSC was linearly related to a higher stress rate as long as the rock deformed elastically, while this relationship became non-linear once the deformation moves in the plastic field prior to brittle failure.

Although our results are still preliminary, our findings can be considered pioneering in the context of the studies devoted to the long-term deformation processes, since no study has been performed in the investigation between geoelectrical signals and long-term crustal deformation phenomena so far. Therefore, further studies of the properties of geoelectrical signals

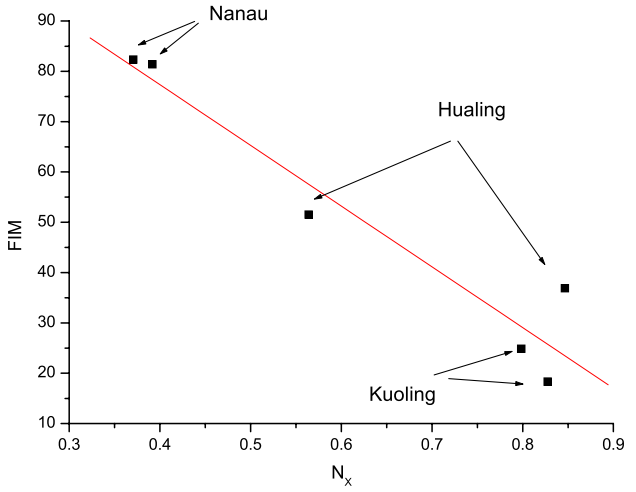

Fig. 12. FS plane for the six signals shown in Fig. 9.

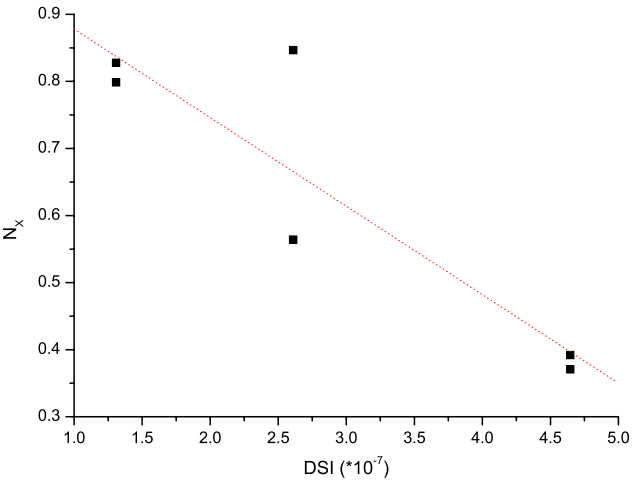

Fig. 13. Relationship between the Shannon entropy power for the signals shown in Fig. 9 and the DSI.

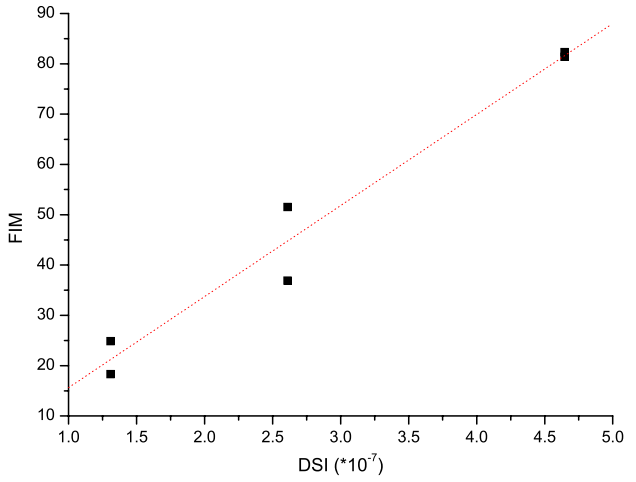

Fig. 14. Relationship between the FIM of the signals shown in Fig. 9 and the DSI.

in Taiwan and different areas would be needed in order to develop a complete physical model that can explain the relationship between the deformation intensity and more ordered structure of geoelectrical signals. The use of the statistical method of Fisher–Shannon surely represents a way to contribute to disclose such connection.

Acknowledgment

The present study was supported by the CNR–NSC Project "Advanced time series analysis tools for magnetotelluric data", in the framework of the Bilateral Agreement for Scientific and Technological Cooperation Between CNR and NSC 2012–2013.

References

[1] S.-B. Yu, H.Y. Chen, L.C. Kuo, Velocity field of GPS stations in the Taiwan area, Tectonophysics 274 (1997) 41–59.
[2] J. Suppe, Kinematics of arc-continent collision, flipping of subduction, and back-arc spreading near Taiwan, Mem. Geol. Soc. China (1984) 21–33.
[3] L.S. Teng, Extensional collapse of the northern Taiwan mountain belt, Geology 24 (1996) 949–952.
[4] F.T. Wu, R.J. Rau, D. Salzberg, Taiwan orogeny: thin-skinned or lithospheric collision? Tectonophysics 274 (1997) 191–220.
[5] C.-P. Chang, T.-Y. Chang, J. Angelier, H. Kao, J.-C. Lee, S.-B. Yu, Strain and stress field in Taiwan oblique convergent system: constraints from GPS observation and tectonic data, Earth Planet. Sci. Lett. 214 (2003) 115–127. http://dx.doi.org/10.1016/S0012-821X(03)00360-1.
[6] A.G. Bos, W. Spakman, M.C.J. Nyst, Surface deformation and tectonic setting of Taiwan inferred from a GPS velocity field, J. Geophys. Res. 108 (2003) 2458. http://dx.doi.org/10.1029/2002JB002336.
[7] Y.-J. Hsu, S.-B. Yu, M. Simmons, L.-C. Kuo, H.-Y. Chen, Interseismic crustal deformation in the Taiwan plate boundary zone revealed by GPS observations, seismicity, and earthquake focal mechanisms, Tectonophysics 479 (2009) 4–18. http://dx.doi.org/10.1016/j.tecto.2008.11.016.
[8] W. Lowrie, Fundamentals of Geophysics, Cambridge University Press, Cambridge, 2007.
[9] M. Moisidi, F. Vallianatos, P. Soupios, S. Kershaw, Spatial spectral variations of microtremors and electrical resistivity tomography surveys for fault determination in southwestern Crete, Greece, J. Geophys. Eng. 9 (2012) 261–270.
[10] P. Soupios, N. Papadopoulos, I. Papadopoulos, M. Kouli, F. Vallianatos, A. Sarris, Th. Manios, Application of integrated methods in mapping waste disposal areas, Environ. Geol. 53 (2007) 661–675.
[11] F. Vallianatos, A. Tzanis, On possible scaling laws between electric earthquake precursors (EEP) and earthquake magnitude, Geophys. Res. Lett. 26 (1999) 2013–2016.
[12] F. Vallianatos, A. Tzanis, A model for the generation of precursory electric and magnetic fields associated with the deformation rate of the earthquake focus, in: M. Hayakawa (Ed.), Seismic Atmospheric & Ionospheric Electromagnetic Phenomena, Terra Scientific Publishing Co., Tokyo, 1999.
[13] P. Varotsos, K. Alexopoulos, Physical properties of the variations of the electric field of the earth preceding earthquakes, I, Tectonophysics 110 (1984) 73–98.
[14] P. Varotsos, K. Alexopoulos, Physical properties of the variations of the electric field of the earth preceding earthquakes, II. Determination of epicentre and magnitude, Tectonophysics 110 (1984) 99–125.
[15] P. Varotsos, K. Alexopoulos, M. Lazaridou, Latest aspects of earthquake prediction in Greece based on Seismic Electric Signals II, Tectonophysics 224 (1993) 1–37.
[16] K. Nomikos, F. Vallianatos, J. Kaliakatsos, S. Sideris, M. Bakatsakis, Latest aspects of telluric and electromagnetic variations associated with shallow and intermediate depth earthquakes in South Aegean, Ann. Geofis. XL 2 (1997) 361–374.
[17] K. Nomikos, F. Vallianatos, Transient electric variations associated with large intermediate-depth earthquakes in South Aegean, Tectonophysics 269 (1997) 171–177.
[18] A. Tzanis, F. Vallianatos, K. Makropoulos, Seismic and electrical precursors to the 17.1.1983 M7 Kefallinia earthquake, Greece: signature of SOC system, Phys. Chem. Earth 25/3 (2000) 281–287.
[19] A. Tzanis, F. Vallianatos, S. Gruszow, Identification and discrimination of transient electric earthquake precursors: fact, fiction and some possibilities, Phys. Earth Planet. Int. 121 (2000) 223–248.
[20] P. Varotsos, The Physics of Seismic Electric Signals, TerraPub, Tokyo, 2005, p. 338.
[21] P.A. Varotsos, N.V. Sarlis, E.S. Skordas, M.S. Lazaridou, Seismic electric signals: an additional fact showing their physical interconnection with seismicity, Tectonophysics 589 (2013) 116–125.
[22] N.V. Sarlis, E.S. Skordas, M.S. Lazaridou, P.A. Varotsos, Investigation of the seismicity after the initiation of a Seismic Electric Signal activity until the main shock, Proc. Japan Acad. 84 (2008) 331–343.
[23] S. Uyeda, T. Nagao, M. Kamogawa, Short-term earthquake prediction: current status of seismo-electromagnetics, Tectonophysics 470 (2009) 205–213.
[24] M.S. Lazaridou, P.A. Varotsos, Earthquake prediction by seismic electric signals, in: The Success of the VAN Method over Thirty Years, Springer, Heidelberg, New York, Dordrecht, London, 2013, p. 251.
[25] F. Vallianatos, A. Tzanis, On the nature, scaling and spectral properties of pre-seismic ULF signals, Nat. Hazards Earth Syst. Sci. 3 (2003) 237–242.
[26] A. Tzanis, F. Vallianatos, A critical review of ULF electric earthquake precursors, Ann. Geofis. 44/2 (2001) 429–460.
[27] F. Vallianatos, D. Triantis, A. Tzanis, C. Anastasiadis, I. Stavrakas, Electric earthquake precursors: from laboratory results to field observations, Phys. Chem. Earth 29 (2004) 339–351.
[28] Q. Huang, Retrospective investigation of geophysical data possibly associated with the *Ms*8.0 Wenchuan earthquake in Sichuan, China J. Asian Earth Sci. 41 (2011) 421–427.
[29] N.R. Lomb, Least-squares frequency analysis of unevenly spaced data, Astrophys. Space Sci. 39 (1976) 447–462.
[30] C.E. Shannon, A mathematical theory of communication, Bell Syst. Tech. J. 379–423 (1948) 623–656.
[31] R.A. Fisher, Theory of statistical estimation, Proc. Cambridge Philos. Soc. 22 (1925) 700–725.
[32] B.R. Frieden, Fisher information, disorder, and the equilibrium distributions of physics, Phys. Rev. A 41 (1990) 4265–4276.
[33] M.T. Martin, J. Perez, A. Plastino, Fisher information and nonlinear dynamics, Physica A 291 (2001) 523–532.
[34] M. Lovallo, L. Telesca, Complexity measures and information planes of X-ray astrophysical sources, J. Stat. Mech. (2011) P03029.
[35] L. Telesca, M. Lovallo, Analysis of the time dynamics in wind records by means of multifractal detrended fluctuation analysis and the Fisher–Shannon information plane, J. Stat. Mech. (2011) P07001.
[36] L. Telesca, M. Lovallo, R. Carniel, Time-dependent Fisher information measure of volcanic tremor before 5 April 2003 paroxysm at Stromboli volcano, Italy, J. Volcanol. Geotherm. Res. 195 (2010) 78–82.
[37] L. Telesca, M. Lovallo, A. Ramirez-Rojas, F. Angulo-Brown, A nonlinear strategy to reveal seismic precursory signatures in earthquake-related self-potential signals, Physica A 388 (2009) 2036–2040.
[38] L. Telesca, M. Lovallo, A. Chamoli, V.P. Dimri, Fisher–Shannon analysis of seismograms of tsnunamigenic and non-tsnunamigenic earthquakes, Physica A 392 (2013) 3424–3429.
[39] L. Telesca, A. Chamoli, M. Lovallo, T.A. Stabile, Investigating the tsunamigenic potential of earthquakes from the analysis of the informational and multifractal properties of seismograms, Pure Appl. Geophys (2014) http://dx.doi.org/10.1007/s00024-014-0862-3. in press.
[40] L. Devroye, A Course on Density Estimation, Birkhauser, Boston, 1987.
[41] A. Janicki, A. Weron, Simulation and Chaotic Behavior of Stable Stochastic Processes, Marcel Dekker, New York, 1994.

[42] M. Troudi, A.M. Alimi, S. Saoudi, Analytical plug-in method for kernel density estimator applied to genetic neutrality study, EURASIP J. Adv. Signal Process. 2008 (2008) Article ID 739082.
[43] V.C. Raykar, R. Duraiswami, 2006. Fast optimal bandwidth selection for kernel density estimation, in: Proceedings of the Sixth SIAM International Conference on Data Mining, Bethesda, April 2006, pp. 524–528.
[44] D. Eccles, P.R. Sammonds, O.C. Clint, Laboratory studies of electrical potential during rock failure, Int. J. Rock Mech. Min. Sci. 42 (2005) 933–949. http://dx.doi.org/10.1016/j.ijrmms.2005.05.018.
[45] P.A. Varotsos, N.V. Sarlis, E.S. Skordas, Electric fields that arrive before the time derivative of the magnetic field prior to major earthquakes, Phys. Rev. Lett. 91 (2003) 148501.
[46] H. Ren, X. Chen, Q. Huang, Numerical simulation of coseismic electromagnetic fields associated with seismic waves due to finite faulting in porous media, Geophys. J. Int. 188 (2012) 925–944.
[47] Q. Huang, One possible generation mechanism of co-seismic electric signals, Proc. Japan Acad. B 78 (2002) 173–178.
[48] F. Vallianatos, A. Tzanis, Electric current generation associated with the deformation rate of a solid: preseismic and coseismic signals, Phys. Chem. Earth 23/9–10 (1998) 933–939.